HHS Public Access

Author manuscript

Hear Res. Author manuscript; available in PMC 2018 July 12.

Published in final edited form as:

Hear Res. 2016 November ; 341: 19–30. doi:10.1016/j.heares.2016.07.018.

Controlled Exploration of the Effects of Conductive Hearing Loss on Wideband Acoustic Immittance in Human Cadaveric Preparations

Gabrielle R. Merchant[1,2], **Saumil N. Merchant**[2,3], **John J. Rosowski**[1,2,3], and **Hideko Heidi Nakajima**[1,2,3]

[1]Harvard-MIT Division of Health Sciences and Technology, Speech and Hearing Bioscience and Technology, Cambridge, MA

[2]Eaton-Peabody Lab, Massachusetts Eye and Ear, Boston, MA

[3]Department of Otolaryngology, Harvard Medical School, Boston, MA

Abstract

Current clinical practice cannot distinguish, with any degree of certainty, the multiple pathologies that produce conductive hearing loss in patients with an intact tympanic membrane and a well-aerated middle ear without exploratory surgery. The lack of an effective non-surgical diagnostic procedure leads to unnecessary surgery and limits the accuracy of information available during pre-surgical consultations with the patient. A non-invasive measurement to determine the pathology responsible for a conductive hearing loss prior to surgery would be of great value. This work investigates the utility of wideband acoustic immittance (*WAI*), a non-invasive measure of middle-ear mobility, in the differential diagnosis of pathologies responsible for conductive hearing loss.

We focus on determining whether *power reflectance* (*PR),* a derivative of *WAI,* is a possible solution to this problem. *PR* is a measure of the fraction of sound power reflected from the middle ear when a sound stimulus is presented to the ear canal. *PR* and other metrics of middle-ear performance (such as ossicular motion via laser Doppler vibrometry) were measured in well-controlled human temporal bone preparations with simulated pathologies. We report measurements before and after simulation of stapes fixation (n=8), malleus fixation (n=10), ossicular disarticulation (n=10), and superior canal dehiscence (n=8). Our results are consistent with the small set of previously published reflectance measurements made in temporal bones and patients. In this present study, these temporal bone experiments with different middle- and inner-ear pathologies were compared to the initial normal state by analyzing both *WAI* and ossicular motion, demonstrating that *WAI* can be a valuable tool in the diagnosis of conductive hearing loss.

Correspondence concerning this article should be addressed to Gabrielle R. Merchant, 358 N. Pleasant Street, Amherst, MA, 01003. gmerchant@umass.edu.
Gabrielle Merchant is now at Department of Communication Disorders, University of Massachusetts, Amherst.

Keywords

Reflectance; wideband acoustic immittance; conductive hearing loss; middle-ear; stapes fixation; superior canal dehiscence; ossicular disarticulation

1. Introduction

The causes of conductive hearing loss are often difficult to determine despite the frequent presentation of patients with various middle-ear diseases in the clinic (Merchant et al., 1998). The transmission of sound energy to the inner ear is affected by a wide range of factors that involve many segments of the peripheral auditory system: from the ear canal through structures within the inner ear. A pathological change anywhere within this sound transmission path can produce a 'conductive' hearing loss. Current clinical practice falls short in the differential diagnosis of patients with conductive hearing loss when they have an intact tympanic membrane and a well-aerated middle ear. Conductive hearing losses in such middle ears are generally associated with stapes immobilization (commonly called a 'fixation') due to otosclerosis, but can also be caused by a discontinuity in the ossicular chain, fixation of the malleus or incus, or a pathological opening in the bony inner ear wall such as a superior semicircular canal dehiscence (SCD) (Minor et al., 2003; Merchant and Rosowski, 2008). These pathological inner-ear openings are called 'third window' pathologies because they – like the normally occurring oval and round windows – are low-impedance paths for air-conducted sound energy to flow into and out of the cochlea.

In common practice, precise determination of the cause of a conductive hearing loss is not achieved without exploratory middle-ear surgery (Merchant and Rosowski, 2010). Even during surgery, diagnosis can be challenging (e.g. hair fracture of the anterior crus or a lesion near the incudo-malleal joint). A non-invasive measurement that objectively distinguishes among possible ossicular and inner-ear pathologies would be of value as it would (1) aid in preoperative counseling and pre-surgical planning, (2) prevent unnecessary middle-ear surgery in cases of patients with third window pathologies, and (3) help screen patients who should be referred for further time consuming and costly testing such as a high resolution computed tomography (CT) scan and vestibular evoked myogenic potential (VEMP) testing. Furthermore, a sensitive objective indicator of the presence of a canal dehiscence, even in the absence of hearing loss, would be a useful part of the diagnostic workup for these bony defects (Merchant et al., 2015).

Clinicians make limited use of objective assessments of middle-ear mobility in diagnosing middle-ear disease. Recently, measurements of *umbo velocity* using laser-Doppler vibrometry (LDV) and *wideband acoustic immittance* (*WAI*) measured in ear canals over a wide frequency range have been shown to aid in the non-invasive diagnosis of conductive disorders with aerated middle ears, including ossicular fixation, disarticulation, and SCD (e.g. Rosowski et al., 2003; Whittemore et al., 2004; Feeney et al., 2003; Allen et al., 2005; Rosowski et al., 2008; Feeney et al., 2009; Shahnaz et al., 2009a; Shahnaz et al., 2009b; Withnell et al., 2009; Voss et al., 2012; Nakajima et al., 2012; Nakajima et al., 2013; Prieve et al., 2013; Merchant et al., 2015). Collectively, these studies demonstrate that broadband

measurements of middle-ear mobility, including *WAI,* can aid in the non-invasive differential diagnosis of conductive pathologies. However, diseased ears can only be compared to an average population of normal ears, as the “normal” condition for a given pathological ear is unknown. Furthermore, substantial variability exists in *WAI* measurements across normal ears such that the normal range is rather broad (Keefe et al., 1993; Voss and Allen, 1994; Margolis, Saly, and Keefe, 1999; Shahnaz and Bork, 2006; Rosowski et al., 2012), even though small test-retest differences in *PR* in individual ears (Vander Werff et al., 2007; Werner et al., 2010; Rosowski et al., 2012) attest to the reliability of current *WAI* measurement techniques.

Precise measurements of *WAI* and its related quantities made in individual ears *before and after* the development of specific pathologies would provide the most controlled assessment of the effect of the pathology on the measurement. Unfortunately, this is not practical in patients where, typically, only measurements of the pathological states are available. The human temporal bone preparation, on the other hand, enables measurements that can be made on a normal ear with no signs of conductive pathology and also after subsequent manipulation of the ear to simulate specific pathologies. Furthermore, reversal of the manipulation can ensure that measured changes were indeed caused by the manipulation. Temporal bone studies enable detailed assessment of the effect of pathology on measurements such as *WAI.*

Limited *WAI* measurements have been published on temporal-bone preparations simulating various middle-ear pathologies including positive and negative static pressure, middle-ear fluid, ossicular fixations, ossicular disarticulation, and tympanic-membrane perforations (Feeney et al., 2009; Voss et al., 2012). In the present study, we investigate a more extensive list of pathologies. We also use *LDV* measurements of ossicular sound conduction as independent measures of the normality of the specimens as well as objective measures of the effects of the simulated pathology on sound conduction (Nakajima et al., 2005b; Chien et al., 2007).

2. Research Design and Methods

2.1. Human Temporal Bone Inclusion Criteria

Twenty-five non-identified human cadaveric temporal bones that were normal on microscopic evaluation were collected from donors with no known history of ear disease. Each specimen was either fresh or previously frozen and was prepared no more than 24 hours prior to measurements. If initial velocity measurements suggested abnormality (either because of suspected air or a leak in the cochlea, as determined by the ratio of the stapes velocity to the round window velocity at low frequencies deviating from half cycle phase differences, or abnormal ossicular motion), the bone was not included in this study (Ravicz et al., 2000; Nakajima et al., 2005b; Rosowski et al., 2007). Three bones were determined to have air in the cochlea and eight either had pre-existing abnormalities or were damaged at some point during the experiment and were not used, leaving data from fourteen temporal bones in this report. Figure 1 shows the half cycle low-frequency phase difference between the stapes and the round-window velocities for all fourteen preparations used in this study

(in black), as well as an example of one preparation (in dashed gray) that did not pass the half-cycle criterion indicating intracochlear air or fluid leak.

Preparation of the bone involved opening the facial recess and epitympanum and severing the stapedial tendon to gain access to the malleus, stapes, and round window. Small pieces (~250 μm squares) of reflective tape (consisting of a collection of 20 to 50 μm plastic auto-reflective beads) were placed on the umbo (ear-canal side of the tympanic membrane), the posterior crus of the stapes, and the round window to increase the reflected light intensity for laser-Doppler vibrometry.

2.2. Temporal Bone Manipulations

Initial velocity and *WAI* measurements were made on each bone in the *normal* state, and repeated after each pathological manipulation. The manipulations included: (1) SCD, (2) reversal of the SCD, (3) malleus fixation, (4) reversal of the malleus fixation, (5) stapes fixation, and (6) disarticulation of the incudostapedial joint. Sometimes we performed all of the manipulations sequentially in a single preparation, while in other experiments only a subset of the manipulations was completed. For experiments studying SCD, the first manipulation was to drill an approximately 2mm long, 1mm wide opening into the posterior wall of the superior semicircular canal to simulate an SCD. This SCD size is consistent with a dehiscence that can be found clinically, although SCD size and location varies substantially in clinical populations (Niesten et al., 2014a; Merchant et al., 2015). Drilling was performed while the semicircular canal was immersed in saline to prevent entry of air into the inner ear, and at least 1mm of saline covered the dehiscence at all times. Reversal of the SCD was achieved by patching the dehiscence with Jeltrate ® (dental impression material from Dentsply International, Philadelphia, PA) while carefully preventing the entrance of air into the semicircular canal, as was performed in Pisano et al. (2012) and Niesten et al. (2014b). After this SCD manipulation and reversal, malleus fixation was achieved by applying dental cement between the dried head of the malleus and the superior wall of the epitympanum. The cement was dried, resulting in a rigid cylindrical bar to fix the malleus head in the same manner as in Nakajima et al. (2005b). After rewetting the specimen and completing measurements in the malleus fixed state, the cement bar was gently severed and removed with minimal ossicular motion, to reverse the effect of malleus fixation. After reversing the SCD or malleus fixation, measurements of stapes and umbo velocities as well as *WAI* were compared to the initial normal responses. These control (reversal) measurements ensured that the observed change in velocities and *WAI* were indeed due to SCD or malleus fixation and not due to other change in the state of the specimen that may have occurred. If a significant change between the initial and post-reversal was found, the experiment was terminated. Stapes fixation was achieved by first carefully drying the footplate area followed by covering the footplate with a minimum amount of cyanoacrylate adhesive (Super Glue ®) and/or dental cement (carboxylate dental cement [Durelon], 3M Products) in the same manner as Nakajima et al. (2005b). It was important to apply multiple thin layers of adhesives to completely dry and harden the glue between applications. Although the size and strength of the malleus and stapes fixation manipulations varied across experiments, the measured change from the normal stapes velocity quantified the fixation-induced middle-ear transmission loss (a measure of

conductive loss). Finally, a sharp scalpel was used to transect the incudostapedial joint to model ossicular disarticulation. The lenticular process of the incus was also removed to produce an air gap between the incus and stapes. Neither the stapes fixation nor the disarticulation manipulations were reversible. All temporal bone preparations were frequently flushed with saline to ensure that the preparation remained moist, especially prior to making measurements. Not all manipulations were performed on all specimens; the number used in each manipulation reported here are: stapes fixation (n=8), malleus fixation (n=10), ossicular disarticulation (n=10), and SCD (n=8).

2.3. Velocity Measurements

Laser Doppler Vibrometry quantified umbo, stapes, and round window velocity using methods described previously (Nakajima et al., 2005a&b). Briefly, a speculum was placed in the bony ear canal of the preparation. The sound source and probe-tube microphone were attached to a coupler, which was attached to the speculum. The speculum was sealed to the bony ear-canal remnant with putty, and the top of the fixture, through which we viewed the umbo and directed the laser, was sealed by a transparent coverslip. Sound stimuli were a series of 74 single tones logarithmically spaced between 104 and 18824 Hz presented between 70 and 90 dB SPL. The probe-tube microphone measured the sound pressure in the ear canal approximately 2mm from the umbo. A laser beam from a laser-Doppler vibrometer (Polytec Inc) was focused either through the glass-backed ear coupler onto the reflective tape placed on the umbo of the tympanic membrane or through the open facial recess onto the reflectors placed on the posterior crus of the stapes, round window or cochlear promontory. Measurements of stapes velocity on the posterior crus were made with the laser beam at an angle of 45–60° to the plane of the stapes footplate. No correction was made to compensate for the small differences between the measured velocity and the velocity orthogonal to the plane of the stapes footplate that would be produced by a piston-like motion of the stapes. The normalized umbo velocity (UV) and normalized stapes velocity (SV) were quantified as the ratio of the measured velocity to the measured stimulus sound pressure in the ear canal near the tympanic membrane. SV was our measure of middle-ear sound transmission to the cochlea. Measurements of UV and SV were compared to measurements of the stimulus-induced motion of the petrous bone (measured on the cochlear promontory) to estimate the signal-to-noise ratio (SNR) of our velocity measurements. Only measurements with SNR equal to or greater than 10 dB were used to describe UV and SV.

2.4. WAI Measurements

One derivative of WAI is the pressure reflectance (R), while another is the impedance measured in the ear canal, Z_{EC}. Pressure reflectance (R) is the complex ratio between the reflected pressure wave and the forward pressure wave propagating in a tube or ear canal. Pressure reflectance is related to Z_{EC}, which is calculated from the sound pressure measurement made in the ear canal, by the following equation:

$$R = \frac{Z_{EC} - Z_0}{Z_{EC} + Z_0}, \quad \text{(Eqn. 1)}$$

where Z_0 is the characteristic acoustic impedance of the ear canal at the measurement point that equals the product of the density of air and the propagation velocity of sound divided by the cross-sectional area of the canal at the measurement point. The cross-sectional area used in the calculation of R is often assumed to be a constant approximation equal to the average cross-sectional area of the human ear canal. Other techniques have been used, including estimating the cross-sectional area based on a pressure measurement in the ear canal (Huang, et al., 2000; Keefe, et al., 1993) as well as making silicon molds of the ear canal to determine the precise cross-sectional area at the measurement location (Voss et al., 2008). Variations in ear-canal cross-sectional area in temporal bone preparations have been shown to have small effects on R. Voss and colleagues (2008) compared the three methods described above for defining the cross-sectional area in calculations of R. They concluded that the common assumption of an average area of 0.43 cm^2 provided a more robust estimate of cross-sectional area than the use of an area based on a pressure measurement. They also concluded that variations within an individual ear in either measurement location or ear-canal cross-sectional area estimates resulted in relatively small effects on R (Voss et al., 2008). The average measured ear-canal cross-sectional area in that work, however, turned out to be larger than the constant assumed area often used previously (i.e. they found it to be 0.48 cm^2 versus the common approximation of 0.43 cm^2). However, the differences they found in R as a result of using the measured area versus the constant area were largest when the measurement location was farthest from the tympanic membrane (~2 cm). This is likely due to the fact that the cross-sectional area is smaller, on average, at measurement locations closer to the tympanic membrane. Given that the measurement location we use in this work is closer to the tympanic membrane, we chose to use the common (but potentially smaller than average) approximation 0.43 cm^2 for our calculations of R in this work.

The associated power reflectance (PR) is the square of the magnitude of R, $PR=|R|^2$, and is a real number between 0 and 1 (assuming no otoacoustic emission contribution). $PR=0$ indicates no power is reflected (all power is absorbed) at the eardrum, and $PR=1$ indicates all forward power is reflected back through the ear canal (Keefe et al., 1993; Voss and Allen, 1994). In the case where the ear is actually generating sound (e.g. in spontaneous otoacoustic emissions), PR may have a value greater than 1.0.

Our method for *calculating WAI* in temporal bone specimens was identical to those used to measure patients previously (Nakajima et al., 2012; Rosowski et al., 2012). Briefly, the ear-canal sound pressure was measured from 0.2 through 6 kHz using an Etymotic ER10C probe (containing a sound source and microphone) that was sealed in the ear canal using plastic tubing within a foam tip, and coupled electrically to signal generation and measurement hardware (Mimosa Acoustics ®) controlled by HearID ® (Mimosa Acoustics) software. To calculate Z_{EC}, the Thévenin equivalent of the sound-delivery system and coupled foam ear tip was estimated from a calibration procedure described earlier (Allen, 1986; Keefe et al., 1992; Voss and Allen, 1994; Shahnaz and Bork, 2006; Voss et al., 2008). A single-tip was used for each experiment. The calculated Thévenin equivalent was required to be within acceptable boundaries predetermined by the HearID software in this 0.2 through 6 kHz range before proceeding. If the calibration was not within the acceptable standards, it was repeated and/or the foam tip was replaced. “Poor” calibrations, as determined by these standards built into the HearID software, were most commonly caused by poor coupling

between the plastic tubing in the center of the foam tip and the foam tip itself or small leaks to the outside produced by incomplete expansion of the foam tip within the calibration cavity. Once the ear canal impedance was estimated, R was calculated using Eqn. 1, and PR was set equal to $|R|^2$.

All measurements were completed in a sound-proof booth to reduce noise interference. After successful calibration, the foam tip coupled to the sound source and microphone was placed securely into the bony ear canal of the preparation (Fig. 2). The tip was allowed to expand for 1 minute prior to measurements. The ear canals varied between 1 and 1.5 cm in length in our preparations, and the WAI probe tip was positioned, on average, between 0.75 and 1 cm from the umbo of the TM. (Note that the probe and microphone for WAI measurements differ from those used during measurements of ossicular velocity described above). Z_{EC} (and R) was measured in response to a wideband chirp stimulus at 60 dB SPL (with an averaging time of three seconds, Fast Fourier Transform length of 2,048 points, and sampling rate of 48,000/sec). Five three-second measurements were taken and averaged for each condition of the middle and inner ear.

3. Results

3.1. Initial Normal Measurements

To evaluate the normality of our temporal bones, we compared our PR, UV and SV measurements in temporal bones to previously published measurements in similar preparations. The measured normal UV in the 14 ears reported here compared well with others, e.g. Nakajima et al. (2005b); and the SV generally fit within the normal ranges described by Rosowski et al. (2007). Figure 3 compares our initial normal PR to the normal temporal bone data of Voss et al. (2012). Figure 3A plots PR for each individual and a mean and range of one standard deviation (SD) and Figure 3B compares the median and interquartile range of our data with those of Voss et al. (2012).

Our normal PR measurements were generally near 1 at the lowest frequencies (indicating that most of the power was reflected), and PR decreased with increasing frequency to a minimum around 1kHz, although the magnitude and frequency of this minimum varied considerably among the different preparations. As frequency increased above the frequency of the minimum, the PR increased until around 4kHz (in some ears PR was greater than one near 4 kHz, this is a point of later discussion), and then tended to decrease. These trends were similar to the Voss et al. data (Fig. 3B), although there were some noticeable differences, including lower PR at low frequencies in our data as well as a tendency toward somewhat higher PR around 4 kHz. Our individual measurements also showed less fine structure at higher frequencies than those of Voss, despite the seven point moving average filter used by Voss et al. (2012). These differences could be due to differences in the preparation and how they were measured, e.g., our measurements were made in a sound-proof chamber, our prepared specimens had significantly shorter ear canals than those used by Voss (ours consisted of only the bony portion of the ear canal which ranged from 1 to 1.5 cm compared to the complete ear canals used in Voss, which, while precise lengths were unreported, probably averaged around 2.5 cm), and our prepared specimens had widely

opened middle-ear cavities, whereas Voss's specimens had sealed middle ears. The potential impact of these differences is considered in the discussion.

3.2. Data from a Single Experiment

To demonstrate the effects observed due to simulated pathology, Figure 4 shows the results from a single cadaveric preparation where all pathologies were simulated. This preparation shows many of the trends common to the entire data set. The *WAI* measurements reported include the related acoustic quantities of *PR* (4A), the angle of *R* (4B) and the magnitude and angle of the acoustic impedance measured in the ear canal Z_{EC} (4C & 4D). Velocity measurements included the magnitude and phase of *UV* (4E & 4F) and *SV* (4G & 4H). Comparison of results from the normal state with results after multiple simulated pathologies in the individual bones allowed us to quantify the changes in *WAI* and ossicular velocity caused by pathology in individual ears: a major goal of this work.

For this representative experiment, the frequency response of the initial normal state is plotted in Fig. 4 with black solid lines. The first pathology simulated was *SCD*, plotted with blue solid lines. After SCD, the *PR* (Fig. 4A) showed a slight downward frequency shift compared to normal as the minimum shifted from around 1 kHz to about 700 Hz. The phase of *R* (Fig. 4B) generally remained stable with the exception of an increase in phase from 700 through 1000 Hz and a decrease in phase from 1500 through 3000 Hz. The Z_{EC} magnitude (Fig. 4C) increased between 800 Hz and 2 kHz, while the Z_{EC} phase (Fig. 4D) was similar to normal with a slight shift to lower frequency. The *UV* magnitude showed small increases from 600 Hz to 1 kHz (Fig. 4E), while the phase generally remained stable (Fig. 4F). After reversal of SCD, the measurements generally returned to the original normal responses (black dashed line).

Responses after *malleus fixation* are plotted with orange lines in Fig 4. Malleus fixation increased *PR* (Fig. 4A) from normal measurements below 2000 Hz. The *R* phase (Fig. 4B) increased from normal between 200–1000 Hz, was similar to normal between 1000 and 2000 Hz, and was slightly increased from normal between 2000–5000 Hz. These increases in *R* phase in various frequency ranges could also be described as a shift in the frequency-phase relationship, with the malleus-fixed phase starting to decrease at a higher frequency compared to normal. The Z_{EC} magnitude (Fig. 4C) was increased as compared to normal between 500 and 1500 Hz, decreased between 1500 and 3000 Hz, and was similar to normal above 3000 Hz (generally, these frequency-dependent malleus fixation changes compared to normal are similar to that observed in *PR*). The Z_{EC} phase (Fig. 4D) was decreased from normal below 2000 Hz. Consistent with the inverse relationship between impedance (sound pressure per unit volume velocity) and mobility (linear velocity per unit sound pressure) (Nakajima et al., 2005b), we found decreases in *UV* and *SV* magnitude with malleus fixation when compared to normal below 1 kHz (Figs. 4F and 4H). *UV* and *SV* phase increased as compared to normal for malleus fixation from 700 Hz and 2000 Hz due to shifts to higher frequencies. Reversal of malleus fixation resulted in return of measured responses back to the initial normal states (black dotted lines).

Responses after *stapes fixation* are plotted with red lines in Fig. 4. Stapes fixation produced increases in *PR* (Fig. 4A) from the normal measurement at frequencies below 2000 Hz. (In

this example, the malleus fixation increased *PR* for a wider/higher frequency region as compared to stapes fixation.) The *R* phase (Fig. 4B) for stapes fixation was higher than normal below 750 Hz, less than normal between 750 and 2000 Hz, and higher between 2000–5000 Hz. Similar to malleus fixation, the phase due to stapes fixation started to decrease at a higher frequency than the normal. The Z_{EC} magnitude (Fig. 4C) was increased as compared to normal below 1000 Hz (similar to the increase in *PR* in stapes fixation relative to normal in this same frequency range), was decreased from normal between 1000 and 2000 Hz, and was similar to normal above 2000 Hz. The Z_{EC} phase (Fig. 4D) was slightly decreased from normal below 1000 Hz, and then increased above normal at higher frequencies (Fig. 4D). We found stapes-fixation related decreases in *UV* magnitude below 1 kHz but the decrease was smaller than that produced by malleus fixation (Fig. 4E). In contrast, the effect of stapes fixation on *SV* was larger than the effect of malleus fixation (Fig. 4G). This difference in the effect of the two fixations is consistent with fixations causing larger decreases in the velocity of ossicles that are closer to the site of fixation. *UV* phase increased as compared to normal between 700 Hz and 2000 Hz; the phase of *SV* was not measurable (too low SNR) after stapes fixation.

Responses after *disarticulation* are plotted with green lines in Fig. 4. Disarticulation produced effects that were opposite of fixation, but more dramatic than the effects due to SCD. After disarticulation, the *PR* (Fig. 4A) minimum shifted downward from around 1 kHz (normal) to about 500 Hz (disarticulation). The minimum *PR* value also decreased from 0.21 (normal) to 0.03 (disarticulation). Disarticulation introduced an upward and then slow downward transition in the phase of *R* (Fig. 4B) at a frequency above the minimum in *PR* magnitude (Fig. 4A). Disarticulation also induced a sharp notch in Z_{EC} magnitude (Fig. 4C) at 500 Hz, but little to no change in Z_{EC} phase (Fig. 4D). We also saw an increase in *UV* magnitude (Fig. 4E) as a result of disarticulation, with the peak of this increase around 500 Hz (the frequency of the disarticulation associated minimum in *PR* and Z_{EC} magnitude), and a sharp transition in the phase of *UV* (Fig. 4F) at the same frequency. While both SCD and disarticulation produced changes in similar directions in this preparation, the changes in magnitude, angle and frequency of the extrema were much greater after disarticulation than after SCD.

3.3. Mean effects across experiments

To compare the effect of pathologies across experiments, *changes from the normal condition* were calculated for each manipulation in each specimen; these changes were then averaged across experiments. Figure 5 shows the mean change from normal and the +/− 1 SD range of changes for *PR* (Fig. 5A), *R* phase (Fig. 5B), Z_{EC} magnitude (Fig. 5C), Z_{EC} phase (Fig. 5D), *UV* magnitude (Fig. 5E), and *UV* phase (Fig. 5F). The changes are plotted for SCD (blue), malleus fixation (orange), stapes fixation (red) and disarticulation (green). The mean change for the reversal back to normal after the SCD (black dashed) and malleus fixation (black dotted) are also shown.

The average changes illustrated in Figure 5 were consistent with many of the changes observed in the representative experiment (Fig. 4), and were the focus of our attempts to determine the effects of the different pathologies on *R*, *PR*, and *UV* measurements. One

obvious difference between these means and the representative measurements was the decrease in size and sharpness of the *PR* minimum (or notch) and *UV* peak induced by ossicular disarticulation and by SCD (Figs. 4A, 5A). There are some small differences observed in the individual data, such as the differences between malleus and stapes fixation in the representative experiment between 250 and 750 Hz in Fig. 4, that are not readily observable in the mean data. The differences are due to the mean data being smoothed because of the averaging of individual measurements with small differences in the frequency ranges and magnitudes of the manipulation induced changes. Furthermore, while ossicular interruption and (to a lesser degree) dehiscence are all-or-nothing effects, variations in the efficacy of the fixation procedures (e.g. Nakajima et al. 2005a&b, see also Fig. 6 and the Discussion) add to the variable effects of these manipulations. Nonetheless, as observed in the means, there is much similarity in the effect of these manipulations on our measurements in individual ears.

Overall, fixation of either the malleus or stapes caused increases in the mean *PR* and Z_{EC} magnitude and decreases in mean *UV* magnitude below 1 kHz (Figs. 5A, C and E). The increase in *PR* due to malleus fixation affected frequencies up to slightly above 2 kHz, while the increase due to stapes fixation affected frequencies up to slightly below 2 kHz (Fig. 5A). This difference in frequency region of effect was also seen in individual experiments (e.g. Fig. 4A). There were also some changes in fine structure (e.g. a notch-like shape around 500 Hz in the *PR* after malleus fixation in the representative example of Fig. 4) not evident in the mean data. The mean phase of *R* was slightly increased by fixation (leading the normal case) below 1000 Hz and slightly decreased (lagging the normal case) above 1000 Hz, although the decreases above 1000 Hz were larger for stapes fixation than malleus fixation (Fig. 5B). The frequency region (1.2–2 kHz) where Z_{EC} transitioned from increasing to decreasing magnitude due to stapes fixation was broader than due to malleus fixation (Fig. 5C). For both fixations, mean Z_{EC} phase was decreased slightly from normal below 1600 Hz and increased slightly from normal above 1600 Hz (Fig. 5D). Fixations also resulted in mean *UV* phase increases between 700 Hz and 2000 Hz (Fig. 5F).

Disarticulation resulted in a decrease in both mean *PR* and mean Z_{EC} magnitude from normal below 800 Hz with a notch in mean *PR* near 500 Hz, followed by an increase in PR and Z_{EC} from normal between 1000 and 2000 Hz (Fig. 5A and C). The mean phase of *R* decreased above 800 Hz, but the mean Z_{EC} phase had slight decrease above 500 Hz (Fig. 5B and D). Disarticulation also caused an increase in the magnitude of mean *UV* below 800 Hz with a decrease in mean *UV* phase between 500 and 5000 Hz.

Average changes due to SCD were similar in direction to those caused by disarticulation, but were smaller in magnitude and slightly higher in frequency. SCD resulted in a decrease in mean *PR* and a very subtle decrease in Z_{EC} magnitude below 800 Hz (Fig. 5A and C). There was evidence of a notch, or minimum, in mean *PR* near 700 Hz (Merchant et al., 2015). Both *PR* and Z_{EC} after SCD were above normal between 1000 and 2000 Hz. SCD caused no significant change from normal in mean *R* phase (Fig. 5B). There was, however, a very slight trend for the Z_{EC} phase to be slightly lower at higher frequencies (above 800 Hz) after SCD. There was a decrease in mean *UV* phase (between 300 and 3000 Hz) due to SCD (Fig. 5F).

3.4. Fixation-Induced Changes in PR and UV Compared to Change in Stapes Velocity

To understand the relationship between the effect that ossicular fixation had on hearing (input to the cochlea as determined by *SV*) and the acoustical and mechanical changes observed in the ear canal with *PR* and *UV*, we compare the changes in *PR* (at 500–700 Hz) and *UV* (at 500 Hz) produced by each fixation with the change in *SV* at 500 Hz (a good indicator of the magnitude of the conductive hearing loss caused by such fixations, e.g. Nakajima et al. 2005a), shown in Figure 6. Our comparison of *UV* and *SV* measurements after fixation (Fig. 6A) is similar to a previously published comparison (Nakajima et al., 2005b). Malleus fixation produced reductions in *UV* magnitude at 500 Hz that were somewhat smaller than the 5 to 35 dB reductions in *SV* magnitude at 500 Hz. Stapes fixations produced 25 to 50 dB decreases in *SV* and much smaller decreases (at most 10 dB) in *UV* (Fig. 6A). In contrast, the two fixations produced similar increases in *PR* magnitude between 500 and 700 Hz (Fig. 6B), despite the smaller reductions in *SV* produced by malleus fixation.

While the different patterns of fixation induced changes in *UV* and hearing loss (as estimated from the change in *SV* magnitude in temporal bones) can separate malleus fixation from stapes fixation in temporal bones or patients (Rosowski et al., 2008; Nakajima et al., 2005a), the similarity of the changes in *PR* produced by the malleus and stapes fixation preclude any *PR*–based separation of these two pathologies. However, our data suggest that the size of the hearing loss (as modeled by the different decreases in *SV* for malleus versus stapes fixation) can help differentiate malleus and stapes fixation. Given that a low-frequency increase in *PR* is consistent with either malleus or stapes fixation, the size of the hearing loss (or, in the case of the temporal bone, the magnitude of *SV*) can help differentiate the two fixations. For example, while similar changes in *PR* were seen for malleus and stapes fixation, stapes fixation generally results in more hearing loss or a larger decrease in *SV*. The combination of *PR* and hearing loss (as demonstrated by the air-bone gap) has been shown to aid in the differential diagnosis of various conductive pathologies in patient populations (Nakajima et al., 2013).

4. Discussion

This work demonstrates the effects of malleus fixation, stapes fixation, disarticulation of the incudostapedial joint, and dehiscence of the superior semicircular canal on measurements of middle-ear function in a well-controlled fresh human temporal bone preparation. The simulated pathologies are representative of pathologies that cause conductive hearing losses in patients with intact tympanic membranes and well-aerated middle ears. Non-invasive pre-surgical diagnosis of the specific pathology responsible for a conductive hearing loss in these patients would be of great value. To this end, understanding how the different pathologies affect functional measurements can help determine whether such measurements accurately predict specific pathologies. Clinical data has limitations: functional measurements in pathological ears can only be compared to population normals, which show wide variations (Keefe et al., 1993; Margolis et al. 1999; Whittemore et al., 2004; Shahnaz and Bork, 2006; Rosowski et al., 2012), that are probably related to significant variations between ears (e.g. the size of the ear canal, the age of the individual, the history of ear

disease, etc.). The temporal bone preparation allows comparisons between initial “normal” measurements in each ear and measurements made after well controlled and defined manipulations that simulate different pathologies, and therefore minimizes the effect of inherent and confounding variations among ears. Furthermore, these preparations allow observations of the effects of reversing the manipulation to better define a causal relationship between manipulation and effect.

4.1. Effects of Manipulation on Mechanics

Figures 4 and 5 demonstrate that at frequencies below 1 kHz both stapes and malleus fixation produce increases in PR and Z_{EC} magnitude, together with decreases in UV magnitude. These effects are consistent with increases in mechanical stiffness due to fixation (Zwislocki and Feldman, 1970). The malleus fixation is reversible; removing the cement between malleus head and the epitympanic wall return the measured PR, Z_{EC}, and UV to the normal values, consistent with the fixation causing the changes in the measurements.

Disarticulation results in relatively sharp decreases (notches) in PR and Z_{EC} magnitude, and increases (peaks) in UV magnitude, near 500 Hz (with some variation in frequencies of notches and peaks). SCD tends to produce smaller peaks in UV magnitude, and smaller notches in PR and Z_{EC} magnitude that all occur at a higher frequency (near 1000 Hz). The notches or peaks are most evident in individual measurements (such as the representative data in Fig. 4). Because the notches (or peaks) occur at slightly different frequencies across ears, averaging smoothens the sharpness and reduces these features (Fig. 5). Averaging can remove important but consistent subtle narrow-band features that occur in individual measurements but vary slightly in frequency; these features in the individual data have the potential to be used for diagnostic purposes, as was shown for SCD as highly sensitive in Merchant et al. (2015).

The presence of the notches and peaks is likely the result of the increasing effects of mechanical resonances in the ear, perhaps due to a decrease in damping at the tympanic membrane, as both a hole in the semicircular canal and a break at the incudostapedial joint decrease the resistive load of the inner ear on the TM (Zwislocki 1962; Moller et al., 1965; Songer and Rosowski 2006 & 2007). Disarticulation also produces an increase in compliance of the middle ear (as the stiffness of the annular ligament no longer constrains the tympanic membrane and remaining ossicles), resulting in a decrease in the ear’s resonant frequency. A similar increase in compliance is not present in the SCD case (as the annular ligament remains intact) and the exposed resonance after disarticulation generally occurs at lower frequencies than those seen after SCD. The decrease in damping introduced by disarticulation is expected to be greater than that caused by SCD, which explains why the notch (or peak) induced by disarticulation is larger in magnitude than the notch (or peak) produced by SCD.

4.2. Comparisons to Published Data

While this is the first time PR measurements of SCD have been made in temporal bones, the SCD-related notches in PR and peaks in UV found in temporal bone experiments are consistent with that found in patient populations (Nakajima et al., 2012; Merchant et al.,

2015). For the ossicular lesions (e.g. malleus fixation, stapes fixation, and disarticulation), similar low-frequency effects on ossicular velocities in temporal bones and patients have been reported in other temporal bone studies. We find similar UV magnitude decreases due to fixation as previously reported in temporal bones, and our comparison of lesion induced changes in SV changes and UV (Figure 6) shows patterns similar to previous reports (Nakajima et al., 2005a&b). We also observed similar changes in PR for both stapes fixation and disarticulation as others have (Feeney et al., 2009; Shahnaz et. al., 2009; Voss et al., 2012).

Differences also exist between our PR results and other published PR data in temporal bones (Fig. 3B). Voss et al. (2012) reported measurements of fixation and disarticulation in temporal bone preparations and observed changes in PR similar to those seen in our temporal bones at frequencies below 2 kHz. However, our normal measurements in temporal bones (Fig. 3B) show differences from measurements of Voss et al. (2012), including a lower PR below 1 kHz, differences in the width of the minimum in reflectance, and differences in the frequency dependence of some of the smaller variations in PR (e.g. we see a peak near 3 kHz, while Voss et al. (2012) shows a peak at a higher frequency). Unlike Voss et al. (2012), our preparation included widely opened middle-ears and mastoid spaces to allow measurements of SV and manipulations of the ossicles. Such an opening removes the compliance of the middle-ear air spaces that restrains the motion of the TM (Zwislocki, 1962; Møller, 1965; Huang et al., 1997), and should result in a decrease in stiffness at the TM and lower PR at low frequencies. Additionally, a closed middle-ear cavity produces additional resonances at frequencies above 2 kHz that add high-frequency fine structure to the middle ear-input impedance and reflectance (Stepp and Voss, 2005; Keefe, 2015). The presence of openings into the cavity, as in our preparation, also adds frequency dependences to the cavity impedance, which differ from those observed in the intact ear (Møller, 1965; Huang et al., 1997). Voss et al. (2008) explored the effects of opening the middle-ear mastoid cavity space and found low frequency decreases in reflectance as well as varied effects at high frequencies. Therefore, sealing the cavity in our specimens might have made our measurements more similar to those of Voss and coworkers.

4.3. Effect of Open Middle-Ear Cavity on Power Reflectance Measurements

We hypothesized that since the open cavity in our preparation is common to our normal and manipulated measurements, that it has little effect on the *changes in PR* (the focus of our analysis) produced by the manipulations. We conducted several control experiments in which we manipulated the cavity condition by repeatedly sealing the cavity with silicone impression material (Westone Silicone Singles ®) and reopening, while we manipulated the ossicular chain. While sealing the cavity in this manner makes our preparation more like that of Voss et al (2012), it does not precisely mimic the live condition. The process of extraction of the temporal bone from the donor, as well as preparing the bone for experiments, often results in an incomplete mastoid cavity with removal of some bone within the mastoid as well as reductions in the air spaces within the mastoid boundaries. This contention is supported by comparisons of measurements of smaller middle-ear/mastoid air volumes in temporal bone preparations where the full mastoid air space is not present (e.g. Voss et al., 2000) with the volume of intact mastoid air spaces (Molvær et al., 1978).

Figure 7A shows *PR* measurements made in a normal temporal bone with an open or closed middle-ear cavity (prior to any simulated pathologies of the ossicles or inner ear). The low-frequency change in *PR* produced by closing the cavity is similar to the difference between our data and that of Voss et al. (2012). However, changes in *PR* produced by our manipulations were generally independent of the state of the middle-ear cavity (Fig. 7B). Such independence is consistent with the cavities only making a small contribution to the stiffness of the human middle ear (Zwislocki 1962).

4.4. The problem of PR calculated to be greater than 1.0

In general *PR* should not exceed 1 in temporal bone preparations where no otoacoustic emissions can be present. Several of our temporal bone preparations exhibit *PR* exceeding 1, usually at the highest frequencies above 4000 Hz where the true *PR* likely approaches 1. Other *PR* measurements made with the same Mimosa measurement system in cadaveric temporal bones have also found incidences where $PR > 1$ (Voss et al., 2008, 2012). Voss et al. (2008 Fig. 7A) shows an example in a single temporal bone where $PR < 1$ with a closed middle ear, but PR > 1 at a high frequency (approximately 2800 Hz) after opening the mastoid space (similar to our preparation). However, the presence of $PR > 1$ at isolated frequencies in other temporal bones with intact middle ears suggests an open cavity is not the source of this artifact. We speculate, as did Voss and colleagues, that PR > 1 is due to small errors in calibration, including errors in the Thévenin equivalent of the transducer and differences between the cross-sectional area of the ear canal and the calibration cavities, that may be exacerbated by the short ear canals in our preparations. It is notable that it is not uncommon for $PR > 1$ at the highest frequencies in patient measurements also made with the same measurement system (Rosowski et al., 2012), even though the relatively high magnitude of the measurement stimuli is not consistent with the presence of large otoacoustic emissions. Another possible contribution to PR >1 is that at high frequency, there is an artifactual pickup of signal at the microphone from the speaker, inherent in the ER10C (Siegel 1995; Scheperle et al., 2008). These issues that can induce PR >1 affect the accuracy of all measurements made with errors in the estimate of the area of the ear canal, or made with the ER10C at frequencies above a few kHz.

4.5. Absolute Data versus Changes from Normal

A potential limitation of focusing on the *changes* from normal produced by a manipulation, as opposed to the absolute data (i.e. the measured power reflectance versus the change in power reflectance from normal), is that in some cases such changes are hard to quantify. A change in measurement is dependent on the *normal* measurement. As *PR* is constrained between 0 and 1, a *high* initial normal *PR* measurement does not allow for significant increases in *PR*. For example, if a patient or temporal bone has a ‘normal’ reflectance that is close to 1 at low frequencies, fixation of the stapes will not produce a large increase in *PR* at low frequencies, because the normal *PR* is already near maximum. Therefore, the *change from normal* in that patient would be very small. However, as our and other data show, even in pathologic ears, there is a wide range of *PR* values that vary across frequency. As demonstrated by Shahnaz et al. (2009a), fixation of the stapes (in cases of otosclerosis) also increases the frequency of the *PR* minimum, and produces large changes in *PR* at frequencies below the minimum.

4.6. Clinical Utility of Power Reflectance, Impedance, and Umbo Velocity

The focus of this work is on the clinical utility of *PR* to enable differential diagnoses of pathologies responsible for conductive hearing loss in the presence of an intact tympanic membrane and well-aerated middle ear. While laser-Doppler vibrometry measurements of ossicular velocity provide useful diagnostic information, there are practical limitations to the use of these measurements as a clinical diagnostic tool (Rosowski et al., 2012). In our hands, *UV* measurements require two well-trained professionals, one of whom can reliably aim the laser on or near the umbo of the tympanic membrane. Additionally, the system is not currently FDA approved for clinical use (only for research purposes), and it is uncertain whether the manufacturer of the laser vibrometry equipment will apply for approval in the near future (Rosowski et al., 2012).

As previously described above, the low frequency changes we observe in ossicular fixations and disarticulations can be related to changes in the stiffness of the ear (Zwislocki and Feldman, 1970). These manipulations affect the impedance in recognizable ways, as stiffness dominates the impedance at frequencies below 1000 Hz, where the bulk of the changes we observe occur (Zwislocki and Feldman, 1970). *PR* is directly related to Z_{EC} and *PR* is calculated from the impedance at the measurement location in the ear canal (as described in the methods). While we find relatively consistent changes due to manipulation in our reported impedance, *PR* has significant advantages as a clinical diagnostic tool over Z_{EC} (e.g. Voss and Allen, 1994; Voss et al., 2008). Z_{EC} is largely influenced by the measurement location due to standing waves in the ear canal, and thus measurement location is crucial when making and interpreting these measurements. If the ear canal acts as a rigid lossless tube, however, then *PR* (and *R* magnitude) is independent of measurement location (Hudde, 1983; Stinson, 1990; Keefe et al., 1993; Voss and Allen 1994; Voss et al., 2008). This is an important consideration for the application of clinical diagnostics, as it is not possible to place the measuring probe tip at a consistent distance from the TM in all patients.

5. Conclusion

To investigate the effects of pathologies that cause conductive hearing loss in the presence of an intact tympanic membrane and well-aerated middle ear in a controlled manner, *PR* and other metrics of middle-ear performance were measured in human temporal bone preparations with simulated pathologies similar to those of the patient populations. These results are consistent with previous studies. The level of control that we obtain in these studies (as opposed to clinical data) allow us to strongly support the clinical observations that conductive disorders change the *PR* in well specified ways and can be used, with other information (e.g. the audiogram), to differentiate conductive pathologies.

Acknowledgments

The authors thank Mike Ravicz who provided software to aid in the administration and analysis of velocity measurements. We also thank Diane Jones who enables our ability to experiment on fresh human temporal bones.

This work was supported by NIH Grant R01 DC004798 and a donation from Mr. Lakshmi Mittal.

All authors contributed extensively to this work. G.R.M. designed and performed experiments, analyzed data, and wrote the paper; S.N.M. aided in conception of the project, provided training in temporal bone dissections

necessary for experiments, and reviewed written portions of the manuscript. J.J.R. and H.H.N. supervised the study from conception to completion, including providing extensive reviews of the manuscript.

Abbreviations

WAI	Wideband Acoustic Immittance
R	Reflectance
PR	Power Reflectance
UV	Normalized Umbo Velocity
SV	Normalized Stapes Velocity
RWV	Round Window Velocity
LDV	Laser-Doppler Vibrometry
SD	Standard Deviation
SNR	signal-to-noise ratio

References

Allen JB. Measurements of eardrum acoustic impedance. In: Allen JB, Hall JH, Hubbard A. , et al., editorsPeripheral Auditory Mechanisms New York, NY: Springer-Verlag; 1986 4451

Allen J, Jeng P, Levitt H. Evaluation of human middle ear function via an acoustic power assessment. J Rehabil Res Dev. 2005; 42:63–78. [PubMed: 16470465]

Beers AN, Shahnaz N, Westerberg BD, Kozak FK. Wideband reflectance in normal Caucasian and Chinese school-aged children and in children with otitis media with effusion. Ear Hear. 2010; 31:221–33. [PubMed: 19858721]

Chien W, Rosowski JJ, Merchant SN. Investigation of the mechanics of type III stapes columella tympanoplasty using laser Doppler vibrometry. Otol Neurotol. 2007; 28:782–787. [PubMed: 17948356]

Feeney M, Grant I, Marryott L. Wideband energy reflectance in adults with middle-ear disorders. J Speech Lang Hear Res. 2003; 46:901–911. [PubMed: 12959468]

Feeney MP, Grant IL, Mills DM. Wideband energy reflectance measurements of ossicular chain discontinuity and repair in human temporal bone. Ear Hear. 2009; 30:391–400. [PubMed: 19424071]

Huang GT, Rosowski JJ, Flandermeyer DT, Lynch TJ, Peake WT. The middle ear of a lion: Comparison of structure and function to domestic cat. J Acoust Soc Am. 1997; 101:1532–1549. [PubMed: 9069624]

Huang GT, Rosowski JJ, Puria S, Peake WT. A noninvasive method for estimating acoustic admittance at the tympanic membrane. J Acoust Soc Am. 2000; 108:1128–1146. [PubMed: 11008815]

Hudde H. Measurement of the eardrum impedance of human ears. J Acoust Soc Am. 1983; 73:242–247. [PubMed: 6826891]

Keefe DH, Ling R, Bulen JC. Method to measure acoustic impedance and reflection coefficient. J Acoust Soc Am. 1992; 91:470–485. [PubMed: 1737890]

Keefe DH, Bulen JC, Arehart KH, Burns EM. Ear-canal impedance and reflection coefficient in human infants and adults. J Acoust Soc Am. 1993; 94:2617–38. [PubMed: 8270739]

Keefe DH, Fitzpatrick D, Liu YW, Sanford CA, Gorga MP. Wideband acoustic-reflex test in a test battery to predict middle-ear dysfunction. Hear Res. 2010; 263:52–65. [PubMed: 19772907]

Keefe DH, Sanford CA, Ellison JC, Fitzpatrick DF, Gorga MP. Wideband aural acoustic absorbance predicts conductive hearing loss in children. Int J Audiol. 2012; 51:880–891. [PubMed: 23072655]

Liu YW, Sanford CA, Ellison JC, Fitzpatrick DF, Gorga MP, Keefe DH. Wideband absorbance tympanometry using pressure sweeps: System development and results on adults with normal hearing. J Acoust Soc Am. 2008; 124:3708–3719. [PubMed: 19206798]

Margolis R, Saly G, Keefe D. Wideband reflectance tympanometry in normal adults. J Acoust Soc Am. 1999; 106(1):265–280. [PubMed: 10420621]

Merchant GR, Roosli C, Niesten MF, Hamade MA, Lee DJ, McKinnon ML, Ulku CH, Roswoski JJ, Merchant SN, Nakajima HH. Power Reflectance as a Screening Tool for the Diagnosis of Superior Semicircular Canal Dehiscence. Otol Neurotol. 2015; 36:172–177. [PubMed: 25076227]

Merchant SN, Ravicz ME, Voss SE, Peake WT, Rosowski JJ. Middle-ear mechanics in normal, diseased and reconstructed ears. J Laryngol Otol. 1998; 112:715–731. [PubMed: 9850313]

Merchant SN, Rosowski JJ. Conductive hearing loss caused by third-window lesions of the inner ear. Otol Neurotol. 2008; 29:282–9. [PubMed: 18223508]

Merchant SN, , Rosowski JJ. Acoustics and Mechanics of the Middle Ear. In: Gulya AJ, Minor LB, , Poe DS, editorsGlasscock-Shambaugh's Surgery of the Ear 6. People's Medical Publishing House-USA, Shelton; CT: 2010 4972

Minor LB, Carey JP, Cremer PD, Lustig LR, Streubel SO, Ruckenstein MJ. Dehiscence of bone overlying the superior canal as a cause of apparent conductive hearing loss. Otol Neurotol. 2003; 24:270–278. [PubMed: 12621343]

Moller AR. An experimental study of the acoustic impedance of the middle ear and its transmission properties. Acta Oto-Laryngol. 1965; 60:129–149.

Molvær O, Vallersnes FM, Kringlebotn M. The size of the middle ear and the mastoid air cells. Acta Oto-Laryngol. 1978; 85:24–32.

Nakajima HH, Ravicz ME, Rosowski JJ, Peake WT, Merchant SN. Experimental and clinical studies of malleus fixation. Laryngoscope. 2005a; 115:147–154. [PubMed: 15630384]

Nakajima HH, Ravicz ME, Merchant SN, Peake WT, Rosowski JJ. Experimental ossicular fixations and the middle ear's response to sound: evidence for a flexible ossicular chain. Hear Res. 2005b; 204:60–77. [PubMed: 15925192]

Nakajima HH, Pisano DV, Roosli C, Hamade MA, Merchant GR, Mafoud L, Halpin CF, Rosowski JJ, Merchant SN. Comparison of ear canal reflectance and umbo velocity in patients with conductive hearing loss. Ear Hear. 2012; 33:35–43. [PubMed: 21857516]

Nakajima HH, Rosowski JJ, Shahnaz N, Voss SE. Assessment of ear disorders using power reflectance. Ear Hear. 2013; 34(7 0 1):48s–53s. [PubMed: 23900180]

Niesten ME, Hamberg LM, Silverman JB, Lou KV, McCall AA, Windsor A, Curtin HD, Herrmann BS, Grolman W, Nakajima HH, Lee DJ. Superior canal dehiscence length and location influences clinical presentation and audiometric and cervical vestibular-evoked myogenic potential testing. Audiol Neurootol. 2014a; 19:97–105. [PubMed: 24434937]

Niesten ME, Stieger C, Lee DJ, Merchant JP, Grolman W, Rosowski JJ, Nakajima HH. Assessment of the effects of superior canal dehiscence location and size on intracochlear sound pressures. Audiol Neurootol. 2014b; 20:62–71. [PubMed: 25531117]

Pisano DV, Niesten ME, Merchant SN, Nakajima HH. The effect of superior semicircular canal dehiscence on intracochlear sound pressures. Audiol Neurootol. 2012; 17:338–348. [PubMed: 22814034]

Prieve BA, Feeney MP, Stenfelt S, Shahnaz N. Prediction of conductive hearing loss using wideband acoustic immittance. Ear Hear. 2013; 34:54s–59s. [PubMed: 23900182]

Ravicz ME, Merchant SN, Rosowski JJ. Effect of freezing and thawing on stapes-cochlear input impedance in human temporal bones. Hear Res. 2000; 150:215–224. [PubMed: 11077205]

Rosowski JJ, Mehta RP, Merchant SN. Diagnostic utility of laser doppler vibrometry in conductive hearing loss with normal tympanic membrane. Otol Neurotol. 2003; 24:165–175. [PubMed: 12621328]

Rosowski JJ, Chien W, Ravicz ME, Merchant SN. Testing a method for quantifying the output of implantable middle ear hearing devices. Audiol Neurotol. 2007; 12:265–276.

Rosowski JJ, Nakajima HH, Merchant SN. Clinical utility of laser-doppler vibrometer measurements in live normal and pathologic human ears. Ear Hear. 2008; 29:3–19. [PubMed: 18091103]

Rosowski JJ, Nakajima HH, Hamade MA, Mafoud L, Merchant GR, Halpin CF, Merchant SN. Ear canal reflectance, umbo velocity and tympanometry in normal hearing adults. Ear Hear. 2012; 33:19–34. [PubMed: 21857517]

Scheperle RA, Neely ST, Kopun JG, Gorga MP. Influence of in situ, sound-level calibration on distortion-product otoacoustic emission variability. JASA. 2008; 124:288–300.

Shahnaz N, Bork K. Wideband reflectance norms for Caucasian and Chinese young adults. Ear Hear. 2006; 27:774–788. [PubMed: 17086086]

Shahnaz N, Bork K, Polka L, Longridge N, Bell D, Westerberg BD. Energy reflectance and tympanometry in normal and otosclerotic ears. Ear Hear. 2009a; 30:219–233. [PubMed: 19194289]

Shahnaz N, Longridge N, Bell D. Wideband energy reflectance patterns in preoperative and post-operative otosclerotic ears. International journal of audiology. 2009b; 48(5):240–247. [PubMed: 19842799]

Siegel JH. Cross-talk in otoacoustic emission probes. Ear Hear. 1995; 16:150–158. [PubMed: 7789666]

Songer JE, Rosowski JJ. The effect of superior-canal opening on middle-ear input admittance and air-conducted stapes velocity in chinchilla. J Acoust Soc Am. 2006; 120:258–269. [PubMed: 16875223]

Songer JE, Rosowski JJ. A mechano-acoustic model of the effect of superior canal dehiscence on hearing in chinchilla. J Acoust Soc Am. 2007; 122:943–950. [PubMed: 17672643]

Stepp CE, Voss SE. Acoustics of the human middle-ear air space. J Acoust Soc Am. 2005; 118:861–871. [PubMed: 16158643]

Stinson MR. Revision of estimates of acoustic energy reflectance at the human eardrum. J Acoust Soc Am. 1990; 88:1773–1778. [PubMed: 2262633]

Vander Werff KR, Prieve BA, Georgantas LM. Test-retest reliability of wideband reflectance measures in infants under screening and diagnostic test conditions. Ear Hear. 2007; 28:669–681. [PubMed: 17804981]

Voss S, Allen J. Measurement of acoustic impedance and reflectance in the human ear canal. J Acoust Soc Am. 1994; 95:372–384. [PubMed: 8120248]

Voss S, Horton NJ, Woodbury RR, Sheffield KN. Sources of variability in reflectance measurements on normal cadaver ears. Ear Hear. 2008; 29:651–665. [PubMed: 18600136]

Voss SE, Merchant GR, Horton NJ. Effects of Middle-Ear Disorders on Power Reflectance Measured in Cadaveric Ear Canals. Ear Hear. 2012; 33:195–208. [PubMed: 22037477]

Voss SE, Rosowski JJ, Merchant SN, Peake WT. Acoustic response of the human middle ear. Hear Res. 2000; 150:43–69. [PubMed: 11077192]

Werner LA, Levi EC, Keefe DH. Ear-canal wideband acoustic transfer functions of adults and two-to nine-month-old infants. Ear Hear. 2010; 31(5):587–598. [PubMed: 20517155]

Whittemore KR, Merchant SN, Poon BB, Rosowski JJ. A normative study of tympanic-membrane motion in humans using a laser-Doppler vibrometer. Hear Res. 2004; 187:85–104. [PubMed: 14698090]

Withnell RH, Parent P, Jeng PS, Allen JB. Using wideband reflectance to measure the impedance of the middle ear. The Hearing Journal. 2009; 62(10):36–38.

Zwislocki J. Analysis of the middle-ear function. 1 Input impedance. J Acoust Soc Am. 1962; 34:1514–1523.

Zwislocki J, , Feldman AS. Acoustic impedance of pathological ears American Speech and Hearing Association; Washington, DC: 1970 ASHA Monographs No. 15

Highlights

- Pathologies that cause CHL affect wideband acoustic immittance (*WAI*) measurements.
- *WAI* show clinical utility in the differential diagnoses of these pathologies.
- *WAI* in normal and pathological ears measured in temporal bones are similar to *WAI* of live humans.

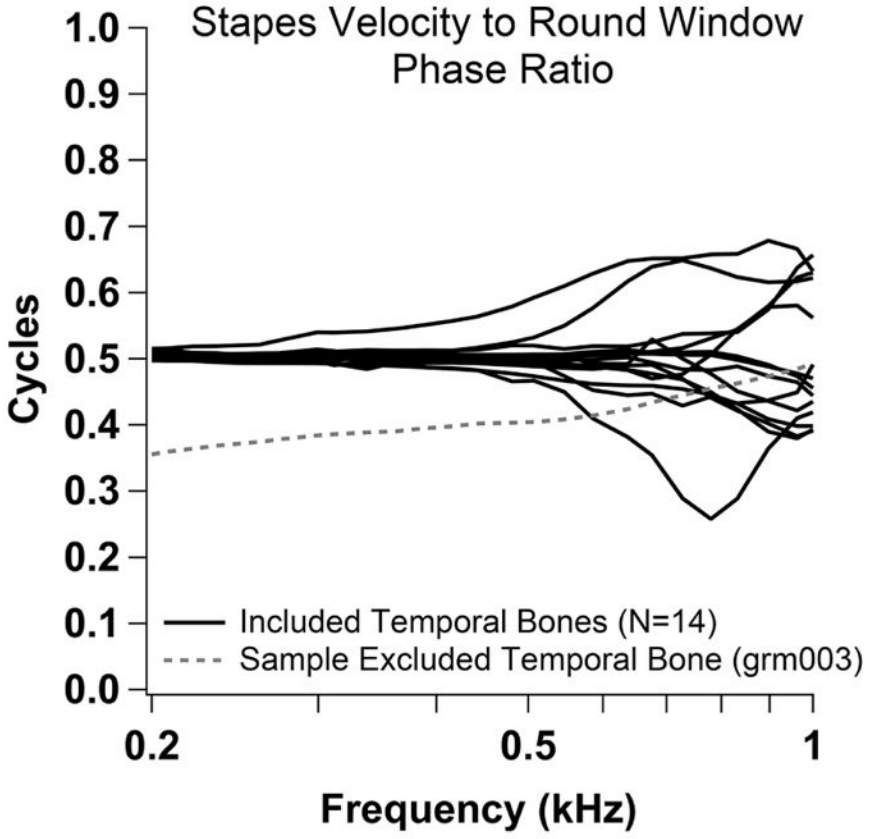

Fig. 1.

Phase ratio between stapes and round window velocity. Half cycle low-frequency phase difference between the stapes velocity and the round window velocity for all fourteen preparations used in this study (black), as well as an example of one preparation (dashed gray) that was excluded due to suspected intracochlear air or fluid leak.

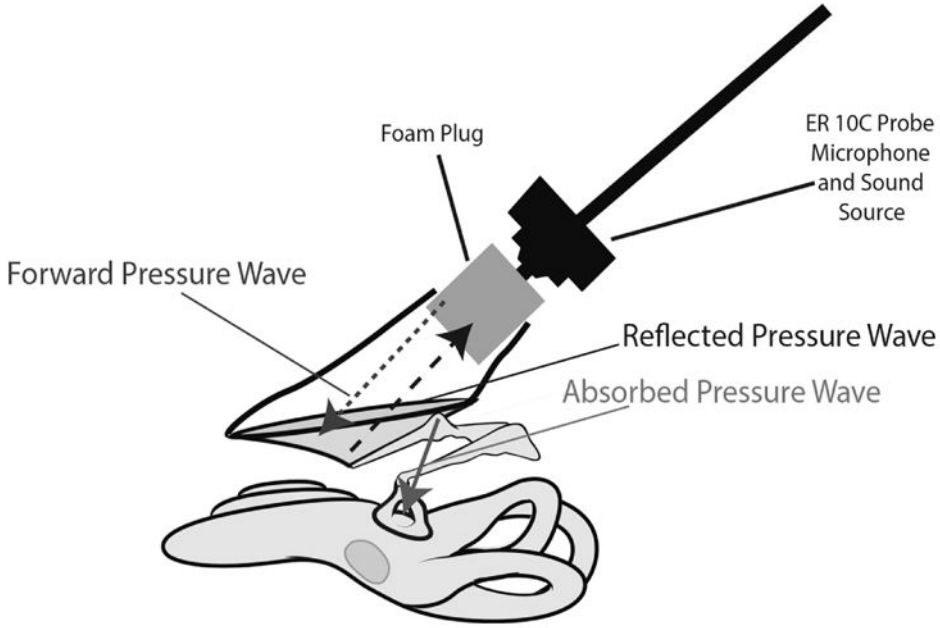

Fig. 2.

Illustration of reflectance measurement. A schematic of the set-up for reflectance measurements in temporal bone preparations, including the sound source, foam plug in the ear canal, tympanic membrane, ossicles and cochlea. The average distance between the medial surface of the foam plug and the tympanic membrane was 1 cm.

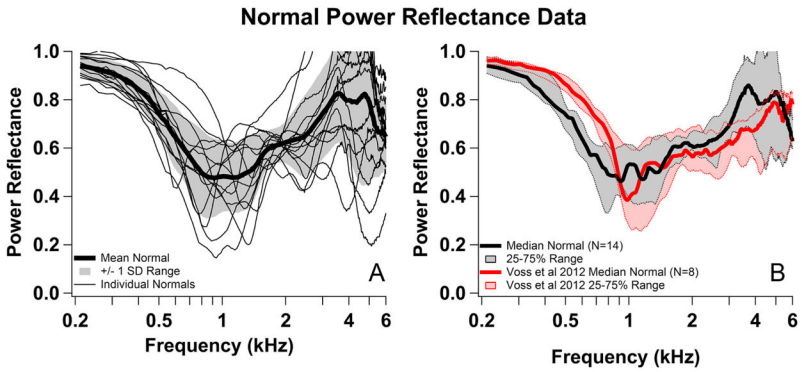

Fig. 3.

Comparisons of normal power reflectance with published data. (A) Normal Power Reflectance (*PR*) measurements for each preparation (n=14) (thin black lines) as well as mean (thick black line) and +/− 1 SD range (gray shading). (B) The median of normal *PR* measurements (thick black line) and 25–75% range (gray shading). Comparison of the median and range from this study (black) and similar median and range from Voss et al. 2012 (red) for normal ears.

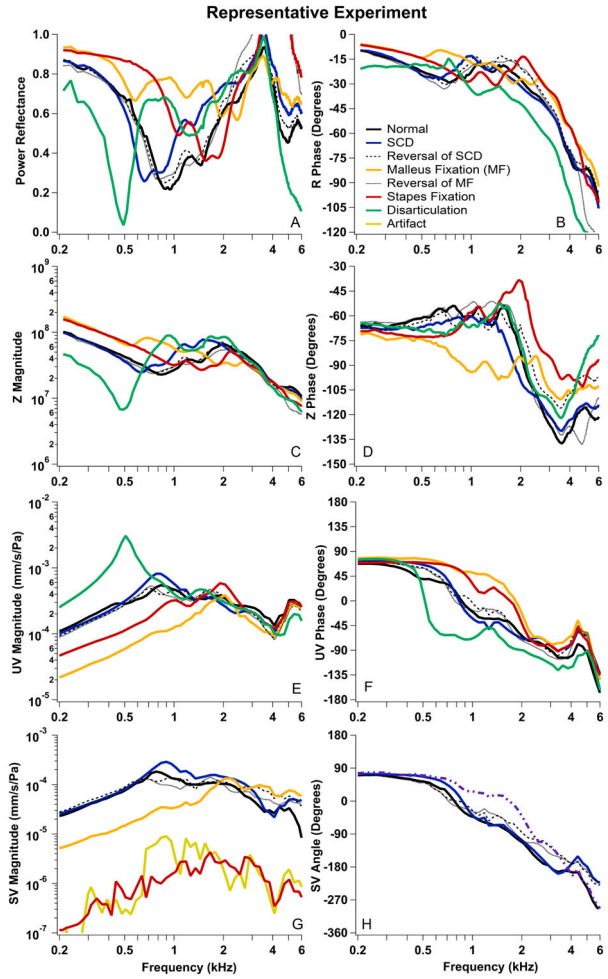

Fig. 4.

Data from one representative experiment in a single cadaveric preparation. (A) Power reflectance (*PR*); (B) Angle of the pressure reflectance (*R*); (C & D) Magnitude and angle of the measured impedance in the ear canal (Z_{EC}); (E & F) Magnitude and angle of the umbo velocity normalized by ear-canal sound pressure (*UV*); (G&H) Magnitude and angle of the Stapes velocity normalized by ear-canal sound pressure (SV). Normal initial measurements are plotted with solid black lines and solid colored lines represent measurements after manipulations (SCD in blue, malleus fixation in orange, stapes fixation in red, and disarticulation in green). Measurements after the reversal of the SCD and malleus fixation manipulations are plotted with black dashed and dotted lines.

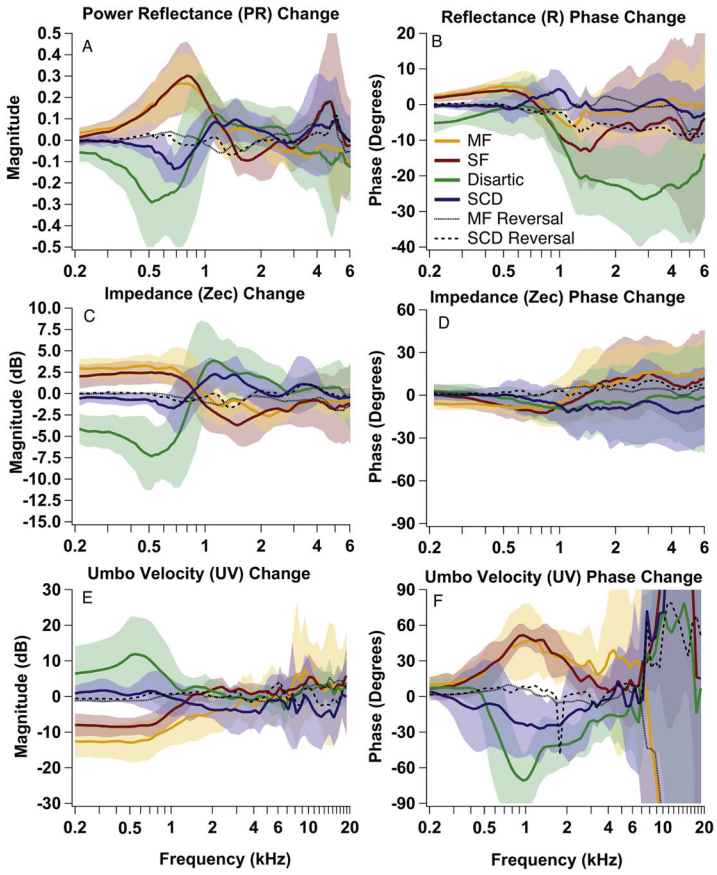

Fig. 5.

Averaged data from all experiments. Mean change from normal (colored lines) +/− 1 SD (shaded area) for *PR* (A), R phase (B), Z_{EC} magnitude and phase (C & D) and *UV* magnitude and phase (E & F) for all manipulation states: SCD (blue), malleus fixation (orange), stapes fixation (red) and disarticulation (green). The mean change for the reversal back to normal after the SCD (black dashed) and malleus fixation (black dotted) are also shown.

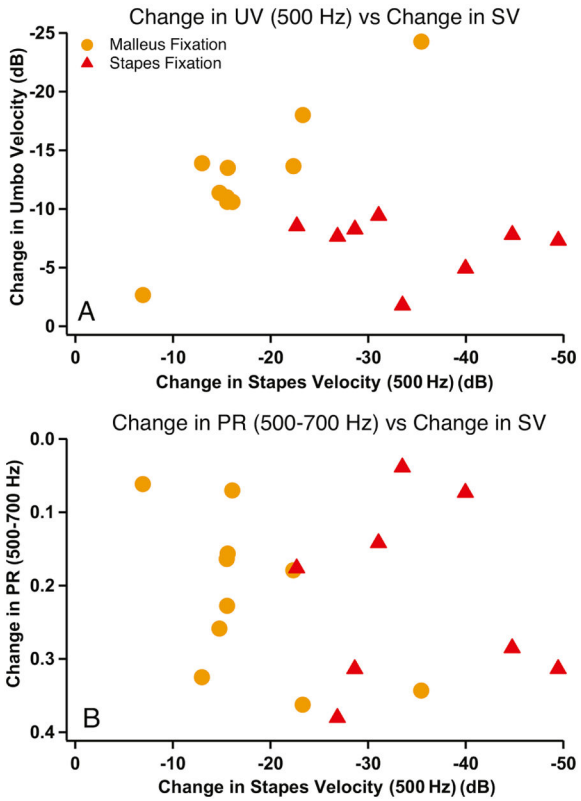

Fig. 6.

Comparison of stapes velocity changes to changes in *PR* and *UV* for malleus fixation (orange) and stapes fixation (red). Comparisons of changes from normal in 500 Hz *UV* (A) and 500–700 Hz *PR* (B) to 500 Hz *SV* changes.

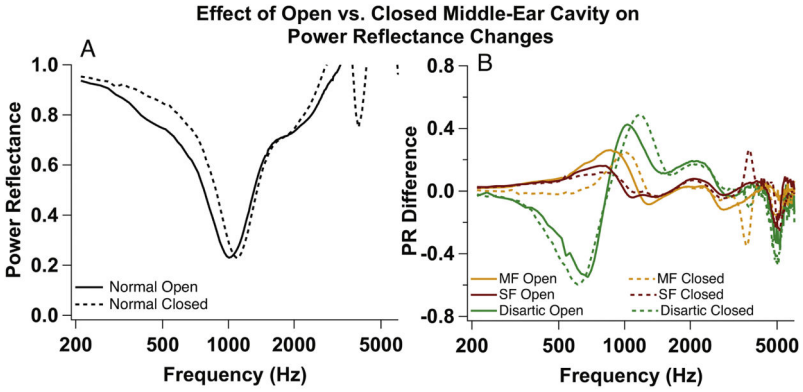

Fig. 7.

Effect of open versus closed middle-ear cavity on *PR*. (A) Measurement made in a normal temporal bone with a cavity widely open (solid) and a sealed cavity (dashed). (B) Difference in *PR* between malleus fixation and normal (MF, orange), stapes fixation (SF, red), and disarticulation (Disartic, green) when cavities are open for all measurements (solid) versus closed for all measurements (dashed).